Development of site-specific antibody-conjugated immunoliposomes for sensitive detection of disease biomarkers

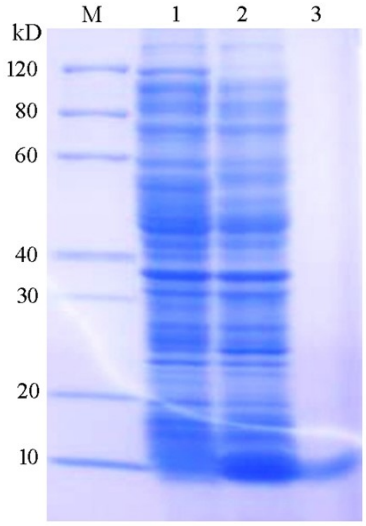

Fig. S1 15% SDS-PAGE assay. Lane 1 shows *E. coli* BL21 (DE3) cells. Lane 2 shows *E. coli* BL21 (DE3) cells harboring pZ_{TAG}–Histag and pEVOL-pBpF plasmids cultured LB medium containing Bpa. Lane 3 shows the purified Z_{Bpa}–Histag by Ni^{2+} affinity chromatography.

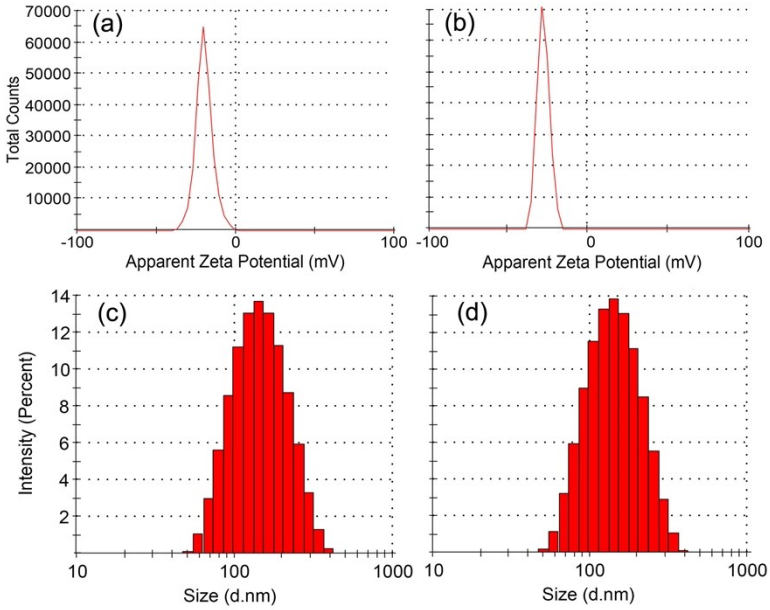

Fig. S2 Zeta potential and size distributions of IgG–*Z-His@HRP-liposomes (a and c) and IgG@HRP-liposomes (b and d).

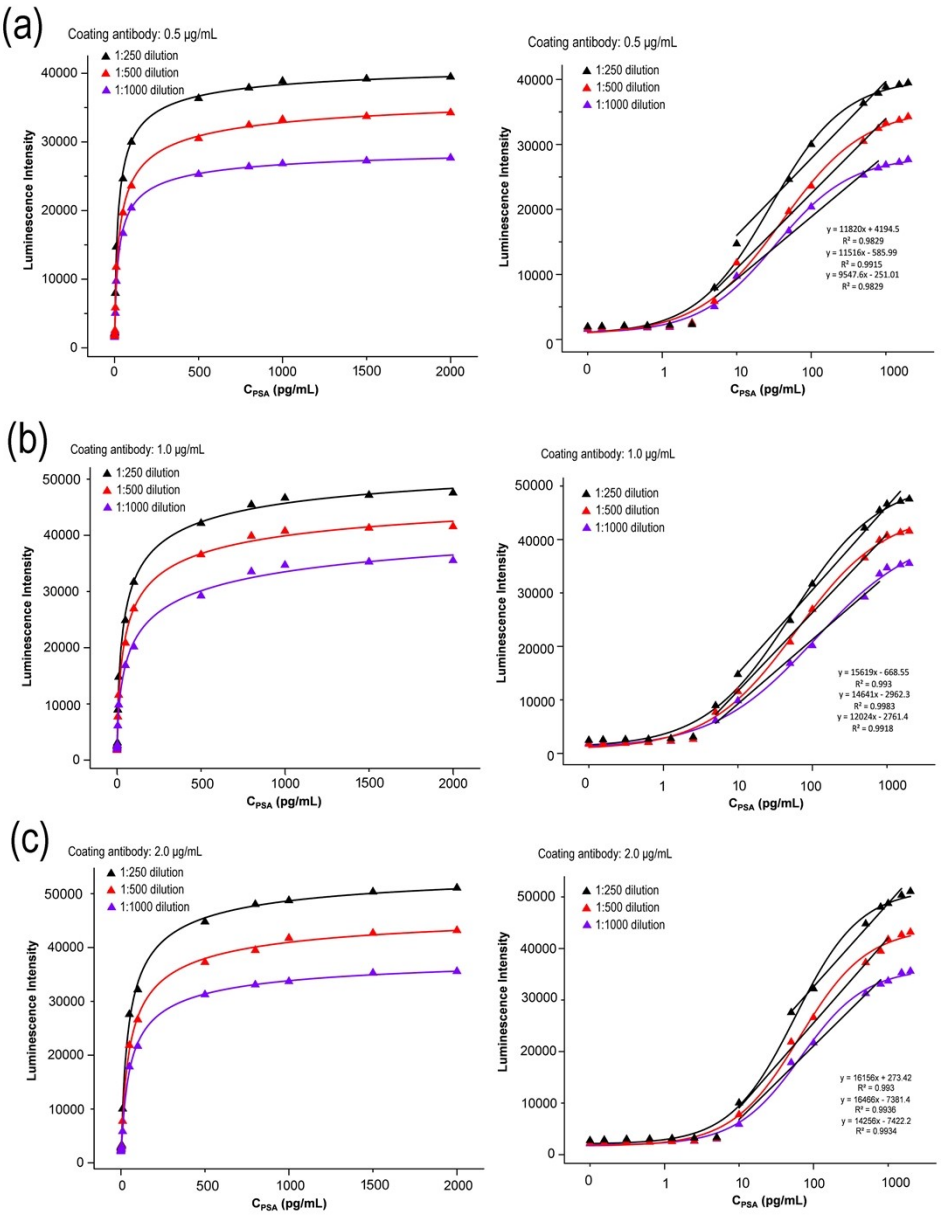

Fig. S3-1 Optimization of the experimental conditions for PSA detection. (a), (b), and (c) show IgG@HRP-liposomes for PSA detection, (d), (e), and (f) show IgG–*Z-His@HRP-liposomes for PSA detection. The response curve of intensities versus PSA concentrations are shown in left, and the calibration curve of intensities versus PSA concentrations are shown in right.

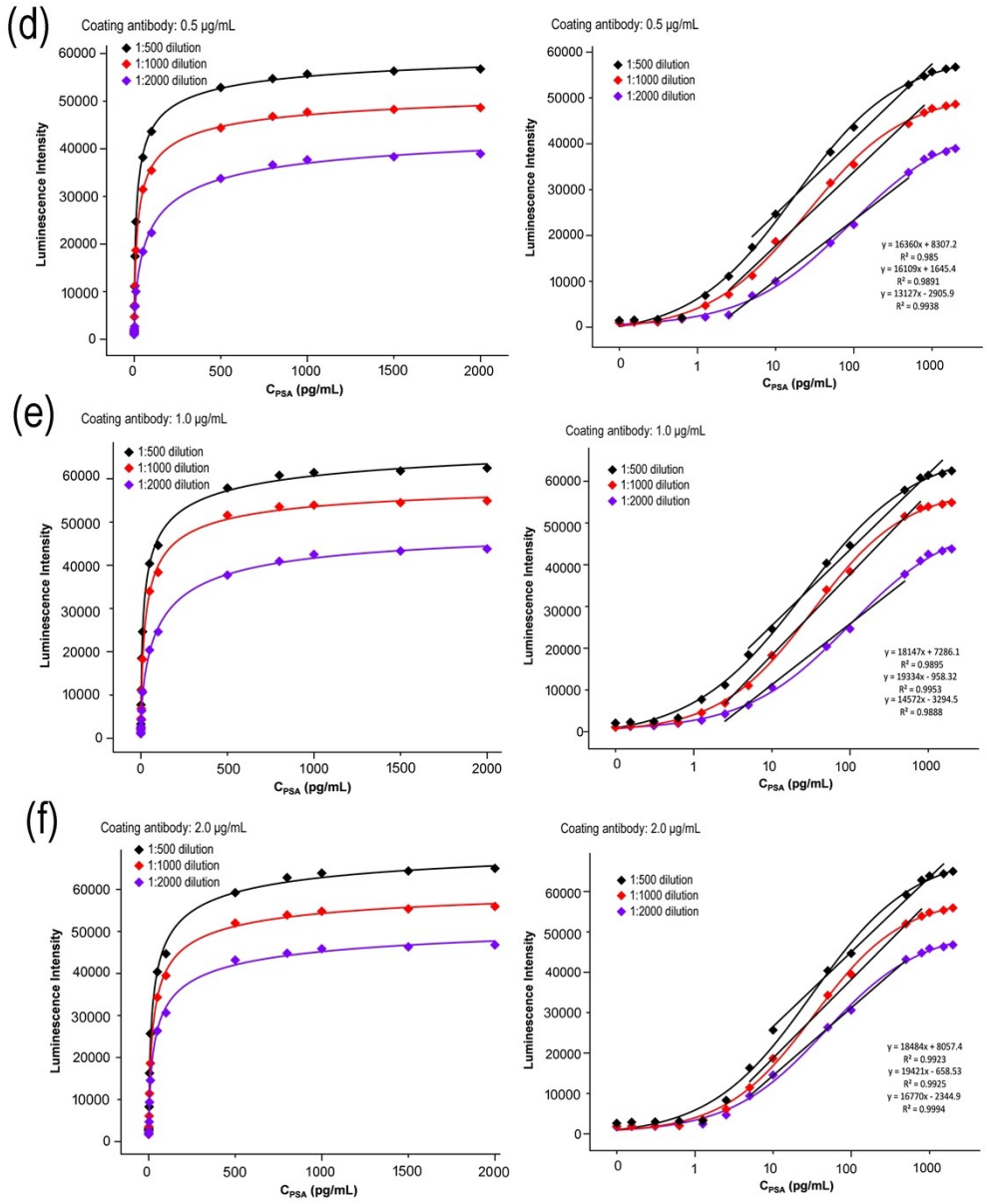

Fig. S3-2 Optimization of the experimental conditions for PSA detection. (a), (b), and (c) show IgG@HRP-liposomes for PSA detection, (d), (e), and (f) show IgG–*Z-His@HRP-liposomes for PSA detection. The response curve of intensities versus PSA concentrations are shown in left, and the calibration curve of intensities versus PSA concentrations are shown in right.

Table S1 The DNA sequences of Z_{Bpa}-Histag fusion protein

sequence
CATATGGTAGACAACAAATTCAACAAAGAACAACAAAACGCGTTCTATGAGATCTAGCATTTACCTAACTTAAACGAAGAACAACGAAACGCCTTCA Z-domain Amber codon TCCAAAGTTTAAAAGATGACCCAAGCCAAAGCGCTAACCTTTTAGCAGAAGCTAAAAAGCTAAATGATGCTCAGGCGCCGAAAGGCGGAGGTGGAT CTGGCGGAGGTGGATCGGGCGGAGGTGGATCACATCATCATCATCATCATTAACTCGAG $(Gly_4\text{-}Ser)_3$Linker Histag

Table S2 LOD (pg/mL) of the optimization on the experimental conditions for PSA detection

Coating antibody	IgG@HRP-liposomes			IgG–*Z-His@HRP-liposomes		
μg/mL	1:1000	1:500	1:250	1:2000	1:1000	1:500
0.5	2.1	2.3	3.5	0.4	0.4	0.6
1	1.4	1.0	3.4	0.3	0.2	0.5
2	3.8	4.1	6.2	1.0	0.8	1.5